

# Nanoscale

Accepted Manuscript



This is an *Accepted Manuscript*, which has been through the Royal Society of Chemistry peer review process and has been accepted for publication.

*Accepted Manuscripts* are published online shortly after acceptance, before technical editing, formatting and proof reading. Using this free service, authors can make their results available to the community, in citable form, before we publish the edited article. We will replace this *Accepted Manuscript* with the edited and formatted *Advance Article* as soon as it is available.

You can find more information about *Accepted Manuscripts* in the [Information for Authors](#).

Please note that technical editing may introduce minor changes to the text and/or graphics, which may alter content. The journal's standard [Terms & Conditions](#) and the [Ethical guidelines](#) still apply. In no event shall the Royal Society of Chemistry be held responsible for any errors or omissions in this *Accepted Manuscript* or any consequences arising from the use of any information it contains.

## COMMUNICATION

## Dumbbell-Like Au-Fe<sub>3</sub>O<sub>4</sub> Nanoparticles: A New Nanostructure for Supercapacitors

Cite this: DOI: 10.1039/x0xx00000x

Sheng Liu,<sup>a,b</sup> Shaojun Guo,<sup>b</sup> Shouheng Sun<sup>b,\*</sup> and Xiao-Zeng You<sup>a,\*</sup>

Received 00th January 2012,  
Accepted 00th January 2012

DOI: 10.1039/x0xx00000x

www.rsc.org/

**Monodispersed dumbbell-like Au-Fe<sub>3</sub>O<sub>4</sub> nanoparticles (NPs) were synthesized and studied for use in supercapacitors. The dumbbell NPs show Au/Fe<sub>3</sub>O<sub>4</sub>-size dependent capacitive behaviors and the 7-14 nm Au-Fe<sub>3</sub>O<sub>4</sub> NPs have the best specific capacitance of 464 F g<sup>-1</sup> at 1 A g<sup>-1</sup> and capacity retention of 86.4% after 1000 cycles, much larger than the pure Fe<sub>3</sub>O<sub>4</sub> NPs (160 F g<sup>-1</sup> and 72.8% retention). This capacitive enhancement is believed to arise from Au-induced increase in electron transfer across the dumbbell-like NPs. The report demonstrates a new strategy to enhance oxide NP capacitance for applications in high performance supercapacitors.**

Rapid increase in energy consumption has stimulated serious inquiries about the sources of energy that is clean and sustainable. Supercapacitor is a popular energy storage device designed to have high power density, long-life cycle and short charge-discharge time.<sup>1-5</sup> To achieve high capacitive performance, its electrodes are better consist of inorganic nanostructured materials, including carbon nanomaterials,<sup>6-8</sup> metal oxide nanoparticles,<sup>9, 10</sup> and metal oxide nanowires/nanotubes.<sup>11, 12</sup> Especially, electrochemically active metal oxides are even more advantageous for charge build-up to reach high capacitance. Fe<sub>3</sub>O<sub>4</sub> is an inexpensive and non-toxic electrode material studied. Due to the stable redox properties of Fe(III)/Fe(II), Fe<sub>3</sub>O<sub>4</sub> is expected to show MnO<sub>2</sub>- or RuO<sub>2</sub>-like pseudocapacitive performance.<sup>13-15</sup> However, pure Fe<sub>3</sub>O<sub>4</sub> exhibit a capacitance only around 100 F g<sup>-1</sup> or less due likely to its surface oxidation (to Fe<sub>2</sub>O<sub>3</sub>) and low electrical conductivity.<sup>16-18</sup> To enhance capacitive performance, Fe<sub>3</sub>O<sub>4</sub> nanostructures can be coupled with a conductive carbon support,<sup>13-15, 19-24</sup> or with a conductive metal.<sup>25-27</sup> For example, when loaded on reduced graphene oxide, Fe<sub>3</sub>O<sub>4</sub> particles show capacitances as high as 480 F g<sup>-1</sup>, the highest value ever reported for Fe<sub>3</sub>O<sub>4</sub>.<sup>20</sup> However, the electrode is made by a spray deposition method and has very limited materials loading for practical applications.

Here we report a new strategy to enhance Fe<sub>3</sub>O<sub>4</sub> nanoparticle (NP) capacitance via dumbbell-like Au-Fe<sub>3</sub>O<sub>4</sub> structure. Dumbbell-like Au-Fe<sub>3</sub>O<sub>4</sub> NPs have been synthesized<sup>28</sup> and studied for catalysis, magnetism and drug delivery because of the unique physical and chemical properties induced by synergetic effect between Au and Fe<sub>3</sub>O<sub>4</sub>.<sup>29-31</sup> Comparing with the commonly studied systems containing

NPs loaded onto a solid support or core/shell structure, the dumbbell Au-Fe<sub>3</sub>O<sub>4</sub> NPs have strong interfacial interactions between the NPs and the support, and have both metal and metal oxide exposed to the electrolyte, realizing effective electron-transfer. Using dumbbell Au-Fe<sub>3</sub>O<sub>4</sub> NPs as an example, we demonstrate that capacitive performance of the structure can be tuned by the sizes of both Au and Fe<sub>3</sub>O<sub>4</sub>, and the capacitance of the 7-14 nm Au-Fe<sub>3</sub>O<sub>4</sub> NPs reaches 464 F g<sup>-1</sup> at 1 A g<sup>-1</sup>.

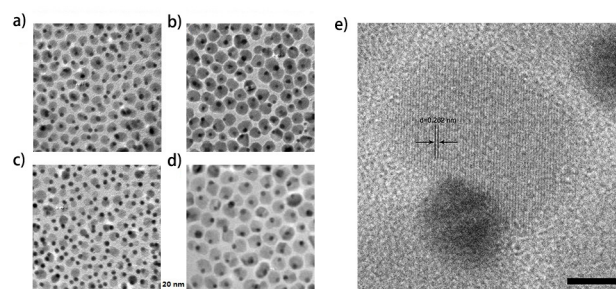


Figure 1. TEM images of the as-synthesized a) 5-14 nm, b) 5-21 nm, c) 7-14 nm, and d) 7-21 nm Au-Fe<sub>3</sub>O<sub>4</sub> NPs. Scale bars: 20 nm. e) HRTEM of a single Au-Fe<sub>3</sub>O<sub>4</sub> NP. Scale bar: 5 nm.

The Au NPs of different sizes (Figure S1a,b) were synthesized by reduction of HAuCl<sub>4</sub>·3H<sub>2</sub>O using borane tert-butylamine (BBA) as reductant.<sup>32</sup> Fe<sub>3</sub>O<sub>4</sub> were then nucleated on these Au seeds by injecting Fe(CO)<sub>5</sub> at 120 °C, followed by heating at 300 °C and air oxidation. The Fe<sub>3</sub>O<sub>4</sub> sizes were controlled by the amount of Fe(CO)<sub>5</sub> injected. Figure 1 a-d shows the TEM images of 5-14 nm, 5-21 nm, 7-14 nm and 7-21 nm Au-Fe<sub>3</sub>O<sub>4</sub> NPs. Figure 1e shows the high-resolution transmission (HRTEM) image of Au-Fe<sub>3</sub>O<sub>4</sub> NPs. Fe<sub>3</sub>O<sub>4</sub> is in single crystalline with the interfringe distance of 0.262 nm, matching the lattice spacing of the (311) planes of Fe<sub>3</sub>O<sub>4</sub>. Single component Fe<sub>3</sub>O<sub>4</sub> NPs (Figure S1c) were also made by etching Au away from the Au-Fe<sub>3</sub>O<sub>4</sub> NPs using KI/I<sub>2</sub> solution as an etching agent and further used as a control.<sup>31</sup> Figure 2 shows the powder XRD patterns of the Au-Fe<sub>3</sub>O<sub>4</sub> and the control Fe<sub>3</sub>O<sub>4</sub> NPs. All the peaks of Au-Fe<sub>3</sub>O<sub>4</sub> match

well with separated Au and Fe<sub>3</sub>O<sub>4</sub> in the powder XRD pattern database indicating that a pure phase was obtained.

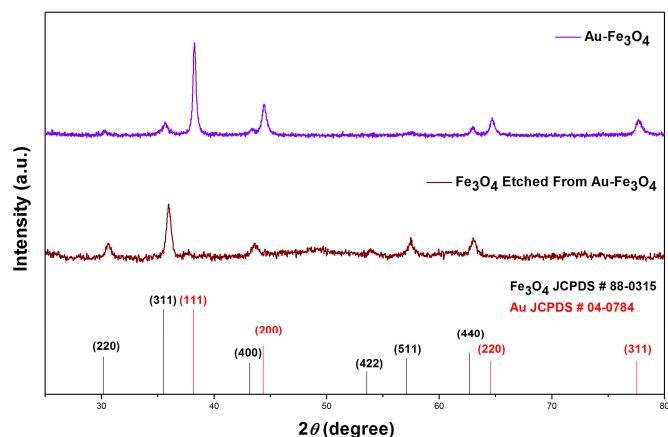


Figure 2. XRD patterns of Au-Fe<sub>3</sub>O<sub>4</sub> NPs, the control Fe<sub>3</sub>O<sub>4</sub> NPs obtained by etching Au away from the Au-Fe<sub>3</sub>O<sub>4</sub> NPs, and the standard (JCPDS) diffraction position of cubic structured Au and Fe<sub>3</sub>O<sub>4</sub>.

To study the capacitive performance of the dumbbell NPs, we deposited these NPs on Ketjen carbon support (Figure S1d), and then mixed the NP-carbon powder with polyvinylidene fluoride (PVDF) in N-methylpyrrolidone (NMP) to form an electrode material paste. We painted the paste onto a Ni foam current collector and analyzed the capacitive behaviors of the NP-electrode. As shown in Figure 3a, the Au-Fe<sub>3</sub>O<sub>4</sub> NPs have a wide potential window from -1.0 V to 0.4 V in 6 M KOH solution which is consistent with previous reports on Fe<sub>3</sub>O<sub>4</sub> NPs.<sup>14</sup> We found that Au-Fe<sub>3</sub>O<sub>4</sub> with different sizes exhibit different charge and discharge times (Figure 3b), which are all significantly longer than the control Fe<sub>3</sub>O<sub>4</sub> NPs, indicating a better performance of the Au-Fe<sub>3</sub>O<sub>4</sub> NPs.

At 1 A g<sup>-1</sup>, the control Fe<sub>3</sub>O<sub>4</sub> NPs show a specific capacitance of 160 F g<sup>-1</sup>, which is higher than the Fe<sub>3</sub>O<sub>4</sub>-carbon systems reported previously,<sup>13, 15</sup> due likely to the high surface area gained from the better controlled Fe<sub>3</sub>O<sub>4</sub> NP size effect. As a comparison, the specific capacitances of the dumbbell NPs are all increased, reaching 464, 383, 302, 255 F g<sup>-1</sup> for the 7-14 nm, 7-21 nm, 5-14 nm, 5-21 nm Au-Fe<sub>3</sub>O<sub>4</sub> NPs, respectively. From the specific capacitance equation,

$$C = \frac{I\Delta t}{m\Delta V} \quad (1)$$

where  $C$  is the specific capacitance,  $I$  is the charge/discharge current,  $\Delta t$  is the discharge time,  $m$  is the mass of active materials on the electrode and  $\Delta V$  is the potential window, we can see when the current density  $\frac{I}{m}$  and potential window  $\Delta V$  remain the same, the specific capacitance  $C$  is only proportional to the discharge time  $\Delta t$ , hence we can compare capacitance of different NPs using their discharge time. Figure 3c and d show the NP size-dependent galvanostatic charge discharge behaviors, from which we see clearly NPs with larger Au and smaller Fe<sub>3</sub>O<sub>4</sub> tend to have better capacitance at 1 A g<sup>-1</sup> and this trend maintains through all the current densities (Figure 3e). Stability tests of the Au-Fe<sub>3</sub>O<sub>4</sub> and the control Fe<sub>3</sub>O<sub>4</sub> NPs at 10 A g<sup>-1</sup> (Figure 3f) indicate that the control Fe<sub>3</sub>O<sub>4</sub> NPs maintain 72.8% of the original capacitance after 1000 cycles while in the same test condition, the Au-Fe<sub>3</sub>O<sub>4</sub> NPs retain much higher capacitance up to 86.4% for the best performed 7-14 nm Au-Fe<sub>3</sub>O<sub>4</sub> NPs.

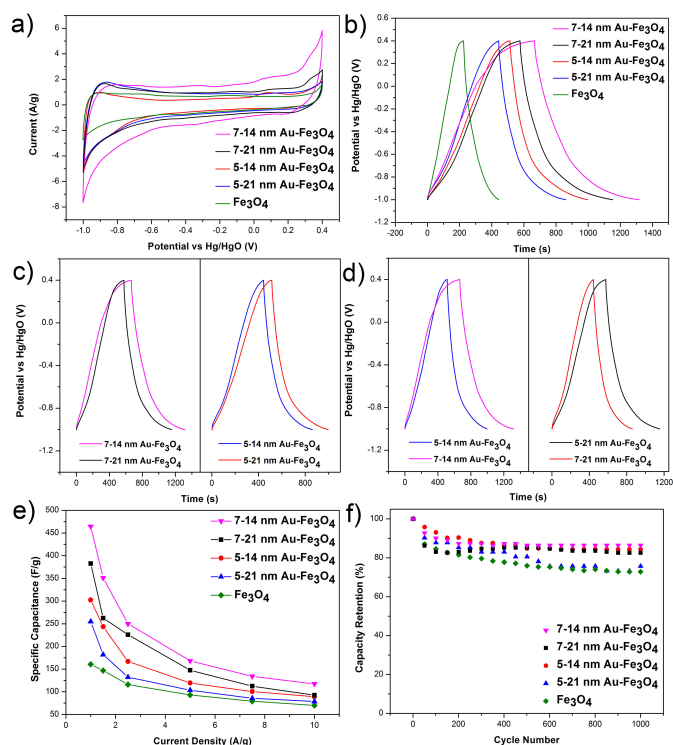


Figure 3. The electrochemistry data of the as-synthesized Au-Fe<sub>3</sub>O<sub>4</sub> NPs and the control Fe<sub>3</sub>O<sub>4</sub> NPs, a) Cyclic voltammograms obtained at the scan rate of 5 mV s<sup>-1</sup>, b) Galvanostatic charge discharge test at 1 A g<sup>-1</sup>, c) Fe<sub>3</sub>O<sub>4</sub> size effect on the galvanostatic charge discharge test at 1 A g<sup>-1</sup>, d) Au size effect on the galvanostatic charge discharge test at 1 A g<sup>-1</sup>, e) Specific capacitance at different current densities and f) the stability test results of the NPs in 1000 cycles.

Table 1. The R<sub>ct</sub> simulated from EIS results.

Sample	R <sub>ct</sub> (Ω)	Sample	R <sub>ct</sub> (Ω)
7-14 nm Au-Fe <sub>3</sub> O <sub>4</sub>	1.73	7-21 nm Au-Fe <sub>3</sub> O <sub>4</sub>	3.51
5-14 nm Au-Fe <sub>3</sub> O <sub>4</sub>	4.49	5-21 nm Au-Fe <sub>3</sub> O <sub>4</sub>	5.77
Control Fe <sub>3</sub> O <sub>4</sub>	9.34		

Since Au is more conductive in the dumbbell NPs, a larger Au/Fe<sub>3</sub>O<sub>4</sub> ratio should lead to a lower resistance and a better capacitance. This was verified by the electrochemistry impedance spectroscopy (EIS) in Figure 4. In EIS study, resistance is divided into two categories: the solution resistance R<sub>s</sub> and the charge transfer resistance R<sub>ct</sub>. As the test condition remains the same, R<sub>s</sub> of different samples are always close to each other. On the other hand, the charge transfer resistance R<sub>ct</sub>, which represents the resistance from the electrode surface to the electrolyte, varies along with the conductivity of the active materials. The equivalent circuit of the supercapacitor can be simulated from the EIS results. As seen in the inner graph of Figure 4, the simulated equivalent circuit consists of a solution resistance R<sub>s</sub>, a charge transfer resistance R<sub>ct</sub> and two constant phase elements QPE<sub>1</sub> and QPE<sub>2</sub>. Simulated R<sub>ct</sub> of all the samples are listed in Table 1. From this Table, we can see that R<sub>ct</sub> of the control Fe<sub>3</sub>O<sub>4</sub> is dramatically larger than that of the Au-Fe<sub>3</sub>O<sub>4</sub> NPs as expected. The dumbbell NPs with larger Au and smaller Fe<sub>3</sub>O<sub>4</sub> have better

conductivity. This study can also explain the capacitive performance differences among all the samples.

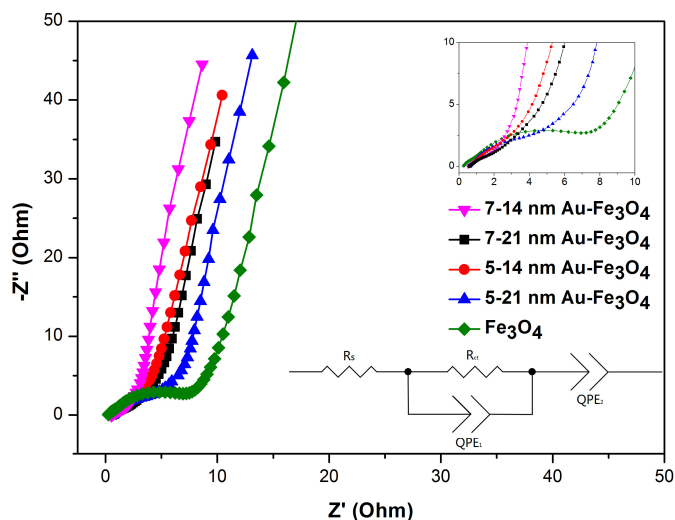
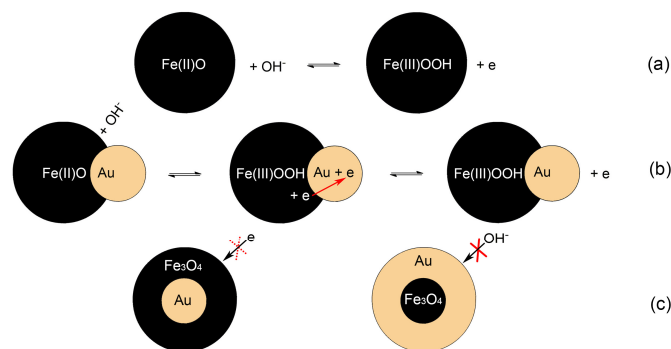


Figure 4. The electrochemical impedance spectroscopy of the as-synthesized Au-Fe<sub>3</sub>O<sub>4</sub> NPs and the control Fe<sub>3</sub>O<sub>4</sub> NPs; simulated equivalent circuit is shown in the inset.



Scheme 1. The proposed energy storage mechanism in (a) pure Fe<sub>3</sub>O<sub>4</sub>; (b) the dumbbell Au-Fe<sub>3</sub>O<sub>4</sub> NPs; and (c) the core/shell NPs.

The capacitance behaviors of the reported NPs are proposed and outlined in Scheme 1. Scheme 1a shows the reaction route from the pure Fe<sub>3</sub>O<sub>4</sub> NPs with their electrochemical behavior dominated by electron transfer from Fe<sub>3</sub>O<sub>4</sub> to electrolyte.<sup>33</sup> When it comes to Au-Fe<sub>3</sub>O<sub>4</sub> NPs, the electron generated from Fe(II) to Fe(III) oxidation can be transferred to Au and further to electrolyte (Scheme 1b). This process can effectively reduce the charge transfer resistance  $R_{ct}$  and hence improve the capacitive performance. This mechanism can also explain why dumbbell NPs are a better choice than the core/shell NPs with either Fe<sub>3</sub>O<sub>4</sub> or Au as a shell (Scheme 1c). When the structure is metal/metal oxide core/shell, because the metal oxide has a relatively poor conductivity, making it difficult for electrons to reach the metal core unless an ultrathin oxide shell is presented.<sup>27</sup> On the other hand, when the metal oxide/metal core/shell structure is present, the electrolyte ion cannot contact the metal oxide surface to initiate the reaction, the capacitance effect are hindered by the metal shell.

## Conclusions

In summary, the current work reports a new idea to enhance Fe<sub>3</sub>O<sub>4</sub> conductivity by forming Au-Fe<sub>3</sub>O<sub>4</sub> dumbbell NPs. By tuning the sizes

of both Au and Fe<sub>3</sub>O<sub>4</sub>, a specific capacitance of 464 F g<sup>-1</sup> is achieved by 7-14 nm Au-Fe<sub>3</sub>O<sub>4</sub> NPs at 1 A g<sup>-1</sup>, which is close to the best capacitive performance ever reported with Fe<sub>3</sub>O<sub>4</sub> as active materials.<sup>20</sup> This methodology can also be applied to other metal oxide like Co<sub>3</sub>O<sub>4</sub>, MnO<sub>2</sub>, and Au may be replaced by Ag, providing a general path to improve the conductivity of transition metal oxides to maximize their capacitive performances.

## Acknowledgements

The work was supported in part by the National Natural Science Foundation of China (21021062, 21271099 and 91022031), National Basic Research Program of China (2013CB922100, and 2011CB808704) and China Scholarship Council.

## Notes and references

<sup>a</sup> State Key Laboratory of Coordination Chemistry, School of Chemistry and Chemical Engineering, Collaborative Innovation Center of Advanced Microstructures, Nanjing University, Nanjing 210093, China

<sup>b</sup> Department of Chemistry, Brown University, Rhode Island 02912, United States

† Electronic Supplementary Information (ESI) available: Experimental details and additional figures (Figure S1 to Figure S4). See DOI: 10.1039/c000000x/

- 1 B. E. Conway, *Electrochemical supercapacitors: Scientific fundamentals and technological applications*, Plenum Press 1999.
- 2 S. Liu, S. Sun and X.-Z. You, *Nanoscale*, 2014, **6**, 2037-2045.
- 3 A. S. Arico, P. Bruce, B. Scrosati, J. M. Tarascon and W. Van Schalkwijk, *Nature Mater.*, 2005, **4**, 366-377.
- 4 R. Kotz and M. Carlen, *Electrochim. Acta*, 2000, **45**, 2483-2498.
- 5 P. Simon and Y. Gogotsi, *Nature Mater.*, 2008, **7**, 845-854.
- 6 L. L. Zhang and X. S. Zhao, *Chem. Soc. Rev.*, 2009, **38**, 2520-2531.
- 7 Y. Zhu, S. Murali, M. D. Stoller, K. J. Ganesh, W. Cai, P. J. Ferreira, A. Pirkle, R. M. Wallace, K. A. Cychoz, M. Thommers, D. Su, E. A. Stach and R. S. Ruoff, *Science*, 2011, **332**, 1537-1541.
- 8 P. Simon and Y. Gogotsi, *Accounts. Chem. Res.*, 2013, **46**, 1094-1103.
- 9 R.-R. Bi, X.-L. Wu, F.-F. Cao, L.-Y. Jiang, Y.-G. Guo and L.-J. Wan, *J. Phys. Chem. C*, 2010, **114**, 2448-2451.
- 10 R. Liu, J. Duay and S. B. Lee, *Acs Nano*, 2010, **4**, 4299-4307.
- 11 J.-H. Kim, K. Zhu, Y. Yan, C. L. Perkins and A. J. Frank, *Nano Lett.*, 2010, **10**, 4099-4104.
- 12 Z. Chen, V. Augustyn, J. Wen, Y. Zhang, M. Shen, B. Dunn and Y. Lu, *Adv. Mater.*, 2011, **23**, 791-795.
- 13 J. Mu, B. Chen, Z. Guo, M. Zhang, Z. Zhang, P. Zhang, C. Shao and Y. Liu, *Nanoscale*, 2011, **3**, 5034-5040.
- 14 Q. Qu, S. Yang and X. Feng, *Adv. Mater.*, 2011, **23**, 5574-5580.
- 15 D. Liu, X. Wang, X. Wang, W. Tian, J. Liu, C. Zhi, D. He, Y. Bando and D. Golberg, *J. Mater. Chem. A*, 2013, **1**, 1952-1955.
- 16 J. Chen, K. Huang and S. Liu, *Electrochim. Acta*, 2009, **55**, 1-5.
- 17 N. L. Wu, S. Y. Wang, C. Y. Han, D. S. Wu and L. R. Shiue, *J. Power Sources*, 2003, **113**, 173-178.
- 18 T. Cottineau, M. Toupin, T. Delahaye, T. Brousse and D. Bélanger, *Appl. Phys. A*, 2006, **82**, 599-606.
- 19 X. Du, C. Wang, M. Chen, Y. Jiao and J. Wang, *J. Phys. Chem. C*, 2009, **113**, 2643-2646.
- 20 W. Shi, J. Zhu, D. H. Sim, Y. Y. Tay, Z. Lu, X. Zhang, Y. Sharma, M. Srinivasan, H. Zhang, H. H. Hng and Q. Yan, *J. Mater. Chem.*, 2011, **21**, 3422-3427.
- 21 A. K. Mishra and S. Ramaprabhu, *J. Phys. Chem. C*, 2011, **115**, 14006-14013.
- 22 A. K. Mishra and S. Ramaprabhu, *J. Phys. Chem. C*, 2010, **114**, 2583-2590.
- 23 Z.-S. Wu, G. Zhou, L.-C. Yin, W. Ren, F. Li and H.-M. Cheng, *Nano Energy*, 2012, **1**, 107-131.
- 24 Y.-H. Kim and S.-J. Park, *Curr. Appl. Phys.*, 2011, **11**, 462-466.
- 25 J. Kang, A. Hirata, L. Kang, X. Zhang, Y. Hou, L. Chen, C. Li, T. Fujita, K. Akagi and M. Chen, *Angew. Chem. Int. Ed.*, 2013, **52**, 1664-1667.
- 26 X. Lang, A. Hirata, T. Fujita and M. Chen, *Nat Nano*, 2011, **6**, 232-236.
- 27 Q. Lu, M. W. Lattanzi, Y. Chen, X. Kou, W. Li, X. Fan, K. M. Unruh, J. G. Chen and J. Q. Xiao, *Angew. Chem. Int. Ed.*, 2011, **50**, 6847-6850.

- 28 H. Yu, M. Chen, P. M. Rice, S. X. Wang, R. L. White and S. Sun, *Nano Lett.*, 2005, **5**, 379-382.
- 29 C. Xu, J. Xie, D. Ho, C. Wang, N. Kohler, E. G. Walsh, J. R. Morgan, Y. E. Chin and S. Sun, *Angew. Chem. Int. Ed.*, 2008, **47**, 173-176.
- 30 C. Xu, B. Wang and S. Sun, *J. Am. Chem. Soc.*, 2009, **131**, 4216-4217.
- 31 Y. Lee, M. A. Garcia, N. A. Frey Huls and S. Sun, *Angew. Chem. Int. Ed.*, 2010, **49**, 1271-1274.
- 32 W. Zhu, R. Michalsky, Ö. Metin, H. Lv, S. Guo, C. J. Wright, X. Sun, A. A. Peterson and S. Sun, *J. Am. Chem. Soc.*, 2013.
- 33 K. Qingqing, T. Chunhua, L. Yanqiong, L. Huajun and W. John, *Mater. Res. Express*, 2014, **1**, 025015.